

Supplemental Files

Interaction of Noncoding RNA with the rDNA Promoter Mediates Recruitment of DNMT3b and Silencing of rRNA Genes

Kerstin-Maike Schmitz*, Christine Mayer*, Anna Postepska, and Ingrid Grummt

This file includes:

Supplemental Materials and Methods

Supplemental Figure Legends S1-S6

Supplemental Figures S1-S6

Supplemental Table S1

Supplemental References

Supplemental Materials and methods

Plasmids and pRNA derivatives

cDNAs encoding TIP5 and TTF-I (Strohner et al. 2001; Evers et al. 1995) and plasmids used to synthesize pRNA and control RNA harboring the multiple cloning site of pBluescript (Mayer et al. 2006) have been published. pRNA-205/-1 harbors murine rDNA sequences from -205 to -1 with respect to the transcription start site. pRNA-113/-39 and pRNA-127/-39 are deletion mutants comprising pRNA sequences from -113 or -127 to -39, respectively. In pRNA/LS-205/-127 sequences upstream of the TIP5 binding site (-127/-39) were replaced by sequences from the multiple cloning site (MCS) of pBluescript SK⁺. pRNA/LS-137/-127 is a linker-scanner mutant in which sequences from -137 to -127 were replaced by foreign sequences. The T₀ element has been deleted in pRNA-ΔT₀, replaced by scrambled nucleotides in pRNA/LS-T₀ and inverted in pRNA/invT₀. In pRNA/pA15, the distance between T₀ and the TIP5 binding region has been increased by insertion of 15 nt (GGTGATCAAGATCTC) at position -135. The rDNA reporter plasmid pMr1930 contains 5'-terminal rDNA sequences (from -1930 to +155). pMr1930ΔT₀ is identical to pMr1930, but essential nucleotides in T₀ have been deleted (Fig. 2A). Sequences of oligonucleotides are listed in Supplementary Table 1. Expression constructs encoding GFP-DNMT1, GFP-DNMT3a, and GFP-DNMT3b were provided by H. Leonhardt, Myc-DNMT1 by T. Kouzarides, and Myc-DNMT3b by C.-L. Hsieh.

Antibodies and siRNAs

Antibodies against TTF-I and TIP5 have been described (Strohner et al. 2001; Evers et al. 1995). Anti-Flag antibodies (M2) were from Sigma, GFP-Trap® from ChromoTek, antibodies against acH4, H3K4me2 and H3K27me3 from Upstate Biotechnology, and anti-HP1α, anti-H4K20me3, anti-DNMTs and anti-GFP antibodies were from Abcam. siRNAs against mouse DNMTs were purchased from Santa Cruz; siRNA against TIP5 and off-target siRNA were from Dharmacon (NM_054078; D-001206-14-20).

Synthesis of pRNA and transfection of pRNA

To synthesize pRNA derivatives, a DNA fragment containing the T7 promoter fused to mouse rDNA sequences from -205 to -1 or the respective mutant sequence was used as a template in T7 RNA polymerase-driven transcription. Control RNA harboring sequences from the multiple cloning site of pBluescript was synthesized by T7 RNA polymerase using

pBluescript SK⁺/*Eco*RI as template. NIH3T3 cells were transfected with 140 pmoles of synthetic pRNA, 200 pmoles of pRNA oligonucleotides or 40 μ moles of siRNA using the Mirus *TransIT* TKO reagent (Mobitec). For ChRIP assays, synthetic pRNA was transfected into cells that were depleted from endogenous pRNA by antisense LNA-DNA gapmers (Mayer et al. 2006). Cells were harvested after 48-68 h and RNA levels were measured by RT-qPCR. The primers used for qPCR are listed in Supplementary Table 1. Transcript levels were normalized to GAPDH mRNA or 28S rRNA.

pRNA knockdown and cell synchronization

3×10^5 NIH3T3 cells were transfected with 50 nM LNA-DNA gapmers (Sigma-Aldrich) in antisense (5'-CAGGtatgacttccaGGTA-3') or sense (5'-TACCtggaagtcataCCTG-3') orientation using the Mirus *TransIT* TKO reagent as described (Mayer et al. 2006). Cellular RNA was isolated 60 h after transfection and knockdown of pRNA was assayed by qRT-PCR using primers -105/-85 and -21/-1. For synchronization, NIH3T3 cells were arrested at G1/S by aphidicolin treatment (2 μ g/ml, 12 h), released into aphidicolin-free medium for 10 h, and cultured for another 14 h in the presence of aphidicolin before release into S-phase in aphidicolin-free medium.

Immunofluorescence

NIH3T3 cells were permeabilized for 3 min with 0.04% Triton X-100 in 20 mM Tris-HCl (pH 7.4), 5 mM MgCl₂, 0.5 mM EDTA, 25% glycerol, and incubated for 30 min with Atto-565 labeled pRNA oligonucleotides in the presence of 25 u/ml RNasin (Promega). Cells were fixed with methanol (7 min) and acetone (1 min) at -20°C, blocked with 1% BSA and immunostained with anti-UBF antibodies. Images were analyzed by confocal microscopy.

Chromatin immunoprecipitation (ChIP), chromatin RNA immunoprecipitation (ChRIP), RNA immunoprecipitation (RIP) and DNA methylation assays

Cells were crosslinked with 1% formaldehyde or were pre-treated with 30 mM 5'-deoxy-azacytidine to trap DNMTs (Schermlle et al. 2005). Chromatin was incubated with antibodies overnight at 4°C and collected with protein A/G-Sepharose for 2 h. Immobilized protein-DNA complexes were washed twice in low salt buffer (150 mM NaCl, 50 mM Tris HCl [pH 8.0], 5 mM MgCl₂ and 1% Triton X-100), twice in the same buffer containing 500 mM NaCl, once in 250 mM LiCl, 10 mM Tris-HCl [pH 8.0], 5 mM EDTA, 0.5% Na-deoxycholate, 0.5% Triton X-100, and twice in TE buffer. After reversal of the crosslink and digestion with

proteinase K, DNA was extracted and amplified by qPCR. The ratio of rDNA in the immunoprecipitates *versus* rDNA in the input chromatin was normalized to control reactions from mock-transfected cells. For ChRIP assays, lysates were supplemented with RNase inhibitors and subjected to ChIP. 5% of the immunoprecipitates were used to quantify precipitated rDNA. RNA was isolated from 95% of the immunoprecipitates and pRNA was analyzed by RT-qPCR. DNA and RNA levels were normalized to *gapdh* and GAPDH mRNA, respectively. Precipitation efficiency was calculated as the percentage of DNA and RNA in the immunoprecipitates compared to the input. Data represent pRNA levels in the immunoprecipitates normalized to precipitated rDNA. For RNA immunoprecipitation (RIP) assays, the respective proteins were immunoprecipitated, co-precipitated RNA was analyzed by RT-qPCR and normalized to GAPDH mRNA or actin mRNA. CpG methylation was monitored by methylation-sensitive restriction enzyme analysis, digesting DNA with *HpaII* before qPCR amplification. The relative amount of *HpaII*-resistant DNA was normalized to mock-digested DNA. Alternatively, CpG methylation was monitored by bisulfite treatment using the EpiTect Bisulfite Kit (Qiagen), amplification and sequencing of rDNA (from -284 to +179).

Electrophoretic mobility shift assays (EMSA)

0.5 pmoles of a ³²P-labeled rDNA promoter fragment (from -205 to -140) were incubated for 5 min on ice with 1-3 pmoles of recombinant TTF-1AN185 in 20 mM Tris-HCl [pH 8.0], 5 mM MgCl₂, 100 mM KCl, 0.2 mM EDTA. After addition of 100 or 250 pmoles of oligoribonucleotides or 10 pmoles of synthetic pRNA and incubation for 15 min, DNA-protein complexes were analyzed on 8% native polyacrylamide gels and visualized by autoradiography.

Southwestern assay

GFP-tagged DNMTs were affinity-purified on GFP-Trap®, separated by SDS-PAGE and transferred to nitrocellulose filters. Proteins were renatured overnight in buffer containing 20 mM Tris-HCl [pH 6.8], 25 mM NaCl, 1 mM EDTA, 10 mM MgCl₂, 0.04% BSA, 0.04% NP40). 150 pmoles of ³²P-labeled triplexes were added, the membrane was incubated for 10 min at room temperature, washed three times, and bound triplexes were monitored by autoradiography.

Supplemental Figure Legends

Figure S1. Ectopic pRNA mediates de novo CpG methylation and transcriptional silencing.

(A) Ectopic pRNA represses rDNA transcription. Left: NIH3T3 cells were transfected with control RNA (ctrl) or pRNA-205/-1 (pRNA) and cellular pRNA levels were quantified by RT-qPCR. Middle: Methylation of the rDNA promoter was determined by methylation-sensitive qPCR, digesting genomic DNA with *HpaII* before PCR amplification. Right: Levels of pre-rRNA and ectopic pRNA were monitored by RT-qPCR. Error bars denote \pm SD ($n \geq 3$).

(B) Bisulfite sequencing of rDNA in NIH3T3 cells transfected with control RNA (top) or pRNA-205/-1 (pRNA; bottom). rDNA sequences from -284 to +179 were amplified, cloned and sequenced. The methylation pattern of 16 representative clones is shown. The CpG residue at position -133 is boxed. Methylated and unmethylated CpG sites are shown as black and white circles, respectively. The numbers refer to the positions of the outermost CpG residues and the transcription start site (arrow).

(C) pRNA alters the chromatin structure at the rDNA promoter. ChIP assay monitoring histone modifications at the rDNA promoter in NIH3T3 cells transfected with control RNA (ctrl) or pRNA-205/-1 (pRNA). Error bars denote \pm SD ($n \geq 2$).

Figure S2. pRNA binds to the T_0 element.

(A) Triplex formation depends on T_0 . Cells were transfected with a control oligoribonucleotide (C) or with pRNA oligo #4 (#4) modified at the 5' end with psoralen and at the 3' end with biotin. Lysates from untreated cells (-) or from cells that were UV-irradiated for 5 min (UV) were incubated with streptavidin-coated magnetic beads and captured DNA was analyzed by qPCR. Bars represent the ratio of captured rDNA to β -actin DNA.

(B) pRNA forms a triple-stranded structure with T_0 . The capture assay was performed as in (A), but lysates were treated with 2 units of RNase V1 (V1) or 15 units of RNase H (H) before incubation with streptavidin-coated beads. The bars represent the relative amount of captured rDNA normalized to *gapdh* DNA. On the right, mock-treated samples were incubated in the absence or presence of *AccI* before qPCR analysis. rDNA levels in *AccI*-digested samples were normalized to rDNA in the undigested samples. Bars represent the level of *AccI*-resistant DNA captured from cells transfected with a control oligo (Ctrl) or pRNA oligo #4, respectively.

(C) Specificity of RNase H and RNase VI for RNA:DNA heteroduplexes and dsRNA, respectively. Left: DNA:RNA heteroduplexes formed by incubating ^{32}P -labeled pRNA with a T_0 -containing DNA oligonucleotide were incubated with RNase H for 30 min (lane 3) before subjecting to EMSA. Right: Double-stranded RNA formed by annealing ^{32}P -labeled pRNA with pRNA in antisense orientation was treated with RNase VI (lane 3).

Figure S3. Triplex formation displaces TTF-I from its target site T_0 .

(A) TTF-I binds RNA. Northwestern blot showing binding of immunopurified GFP-tagged TTF-I to ^{32}P -radiolabeled MCS-RNA (MCS), pRNA-205/-1 (pRNA), or pRNA- ΔT_0 (ΔT_0). Coomassie stained GFP-TTF-I is shown on the right.

(B) TTF-I is associated with pRNA in vivo. GFP-tagged TTF-I was immunoprecipitated from NIH3T3 cells that were transfected with pRNA-205/-1 (pRNA) or with pRNA- ΔT_0 (ΔT_0), and TTF-I associated pRNA was monitored by RT-qPCR. Data represent the level of bound pRNA normalized to GAPDH mRNA.

(C) Triplex formation at T_0 leads to dissociation of TTF-I. NIH3T3 cells were transfected with pRNA oligonucleotides #1 or #4, and rDNA occupancy of TTF-I was assayed by ChIP. Error bars indicate \pm SD ($n \geq 3$).

(D) TTF-I levels do not alter during S-phase progression. NIH3T3 cells were arrested at G1/S by aphidicolin treatment (0h), released into the cell cycle, and TTF-I levels were monitored during S-phase progression. As a control, membranes were reprobed for α -tubulin.

Figure S4. Nucleolar targeting of pRNA is not mediated by DNA:RNA heteroduplexes.

(A) Permeabilized NIH3T3 cells were incubated with Atto-565 labeled pRNA oligo #4 in the absence or presence of RNase H. As a control, oligo #4 was hybridized to a matching DNA oligonucleotide prior to incubation (lower panels).

(B) The confocal image is a magnification of the experiment in Figure 3D, showing colocalization of Atto-565-labeled oligo #4 (red) with immunostained UBF (green) in the nucleolus.

Figure S5. Dnmt1, Dnmt3a and DNMT3b bind RNA.

(A) DNMTs are associated with pRNA in vivo. GFP-tagged TIP5, DNMT3a, DNMT3b and DNMT1 were immunoprecipitated from lysates of HEK293T cells and associated pRNA was monitored by RT-qPCR. Data represent bound pRNA normalized to 28S rRNA.

(B) Northwestern blot demonstrating binding of HIS-mTIP5₁₋₅₉₈, the RNA binding deficient

mutant HIS-mTIP5-ΔMBD₁₋₅₉₈ (Mayer et al., 2006), GFP-tagged DNMT1, DNMT3a and DNMT3b to radiolabeled ³²P-MCS-RNA. The Coomassie stained gel shows the amount of proteins used.

Figure S6. Model of triplex-mediated rDNA methylation and transcriptional silencing.

pRNA (red) forms a triplex structure with T₀, thereby displacing the transcription factor TTF-I from its binding site. The triplex structure targets DNMT3b to the rDNA promoter, leading to methylation of CpG-133 and inhibition of transcription complex assembly. Triplex formation allows the neighbouring hairpin structure of pRNA to bring NoRC close to the rDNA promoter. The interaction of TIP5 with histone deacetylases (HDAC) and histone methyltransferases (HMT) generates a heterochromatic structure that consolidates rDNA repression.

Supplemental Table S1

ChIP and qPCR primers		usage
mrDNA-232//214 For	GAAAGCTATGGGCCGCGGT	H; ChIP
mrDNA-205/-183 For	GACCTGTCGGTCTTATCAGTTC	CA, ChIP,TF
mrDNA-160/140 Rev	CCGGACCTCAAAGGAACAAC	TF
mrDNA-160/140 For	GTTGTTCTTTGAGGTCCGG	ChIP
mrDNA-105/87 For	CCCAGGTATGACTTCCAG	RT-qPCR
mrDNA-105/87 Rev	CTGGAAGTCATACCTGGG	CA, H
mrDNA-21/-1 Rev	ACCTATCTCCAGGTCCAATAG	ChIP, RT-qPCR
GAPDH For	CATGGCCTTCCGTGTTCTTA	RTqPCR
GAPDH Rev	GCGGCACGTCAGATCCA	RTqPCR
mrDNA+597/+619 For	CGTGTAAGACATTCTATCTCG	RTqPCR
mrDNA+745/765 Rev	GCCCGCTGGCAGAACGAGAAG	RTqPCR
TFR oligonucleotides		
Sal box top	AGGTCGACCAGTTGTTCTTTGAGGTCCGG	
Sal box bottom	CCGGACCTCAAAGGAACAACCTGGTCGACCT	
RNA oligonucleotides		
pRNA-oligo #1	GUCGGUCUUAUCAGUUCUCC	
pRNA-oligo #2	UCAGUUCUCCGGGUUGUCAG	
pRNA-oligo #3	GGGUUGUCAGGUCGACCAGU	
pRNA-oligo #4	GUCGACCAGUUGUUCUUG	
pRNA-oligo #5	UGUUCUUGAGGUCCGGUU	
pRNA-oligo #6	AGGUCCGGUUCUUUCGUUA	
pRNA-oligo #7	CUUUUCGUUAUGGGGUCAUU	
Bio-oligo #1	GUCGGUCUUAUCAGUUCUCC	
Bio-oligo #4	UCAGGUCGACCAGUUGUUCUUGAGG	
Psoralen-Bio-oligo ctrl	GUGGGUGGGGGUGGGGGG	
Psoralen-Bio-oligo #4	GGUCGACCAGUUGUUCUUGAGGUCCGGU	
Bisulfite oligonucleotides		
BIS-mrDNA prom FW	GAGTTTTTTTTCTTTTCTTA	
BIS-mrDNA prom RV	CAATTATCACAACTACCCAC	

Table S1: Oligonucleotides used in this study. The sequences are given in 5' to 3' direction. CA, triplex capture assay; H, *HpaII*-sensitive qPCR; TF, triplex formation assay

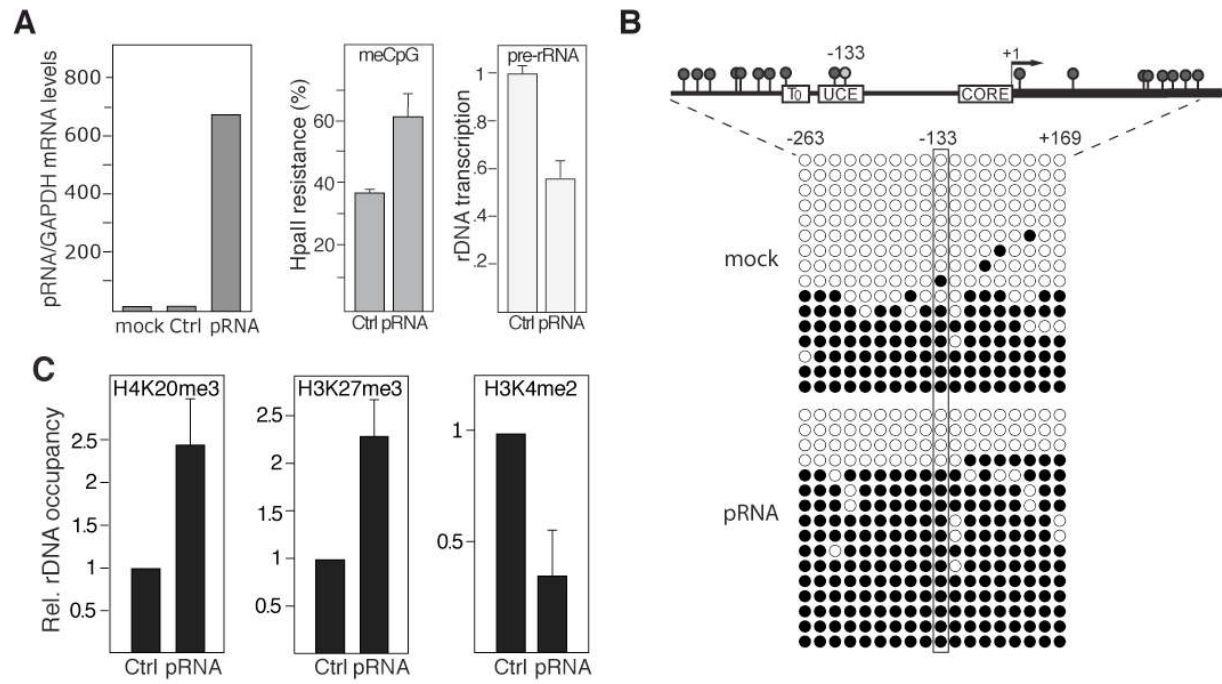
Supplemental References

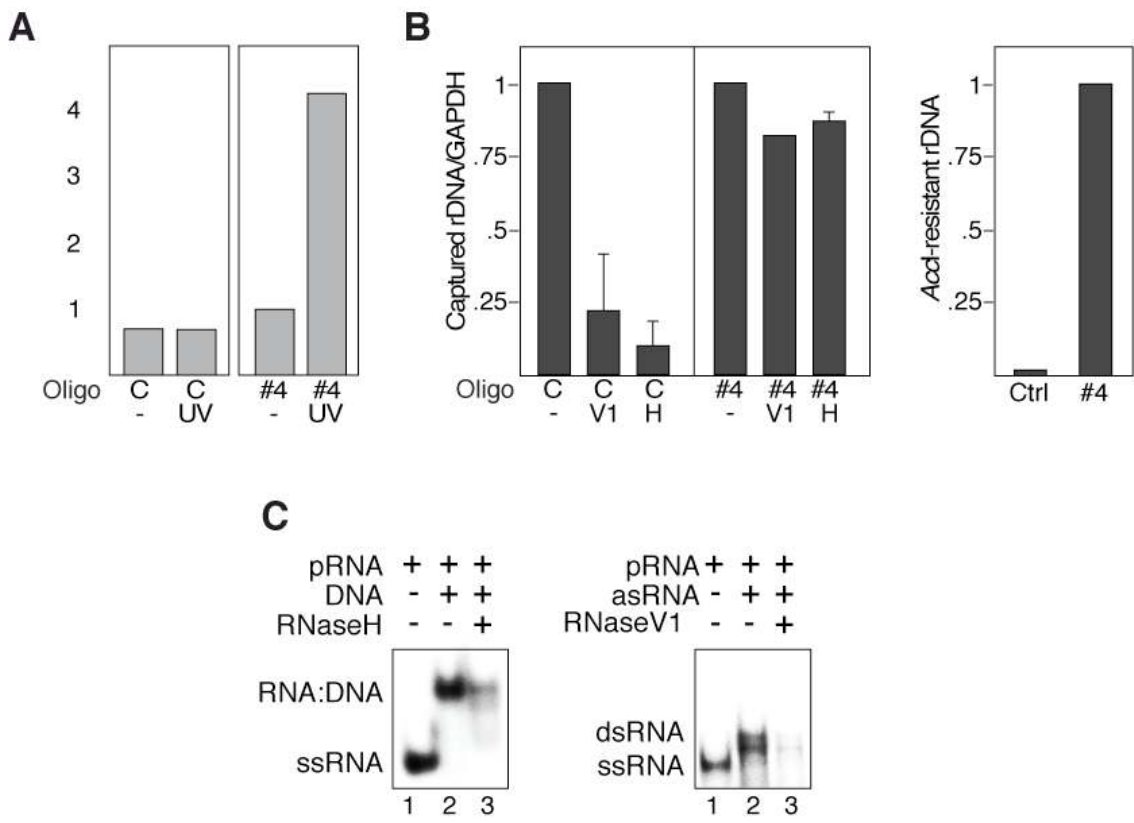
Evers, R., Smid, A., Rudloff, U., Lottspeich, F., and Grummt, I. 1995. Different domains of the murine RNA polymerase I-specific termination factor mTTF-I serve distinct functions in transcription termination. *EMBO J.* **14**: 1248-1256.

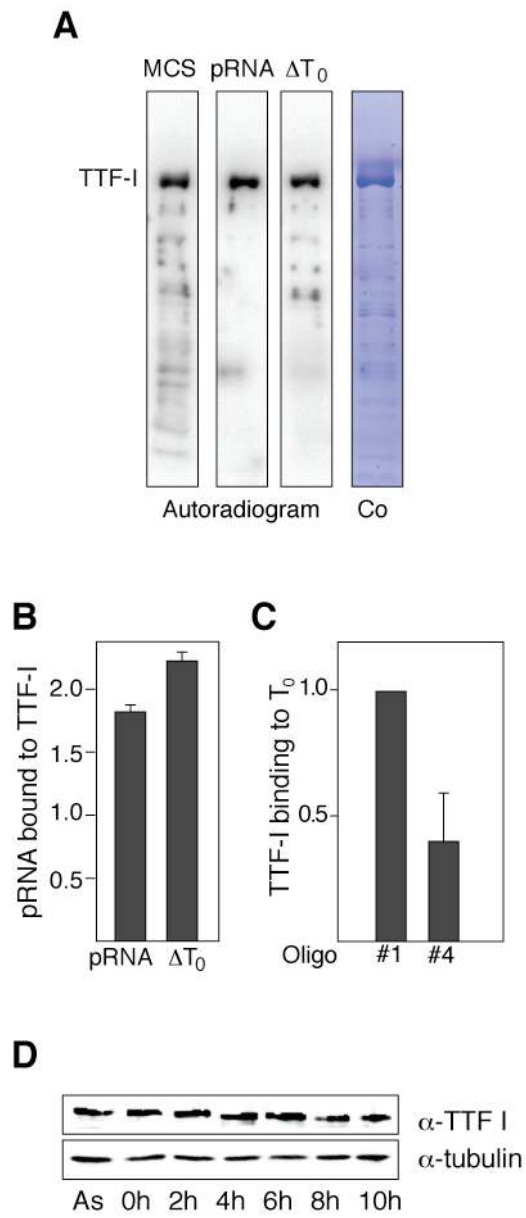
Mayer, C., Schmitz, K.-M., Li, J., Grummt, I., and Santoro, R. 2006. Intergenic transcripts regulate the epigenetic state of rRNA genes. *Mol. Cell* **22**: 351-361.

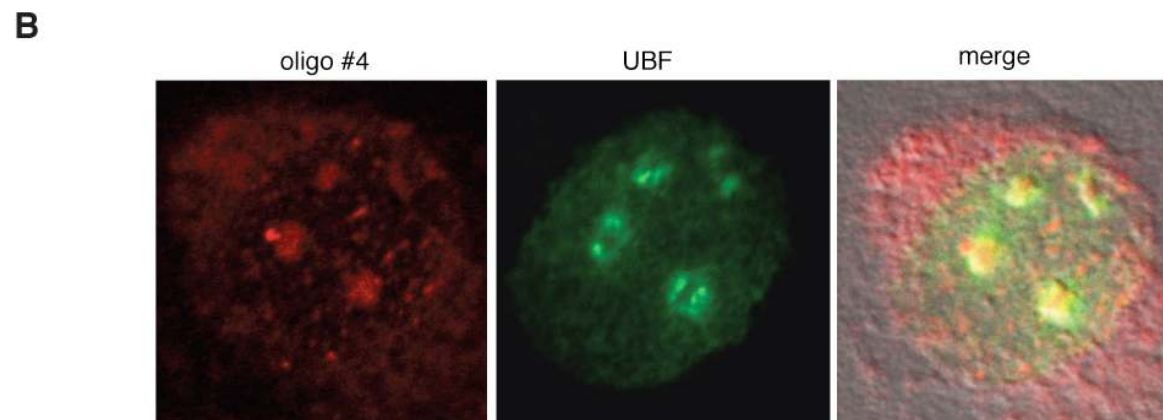
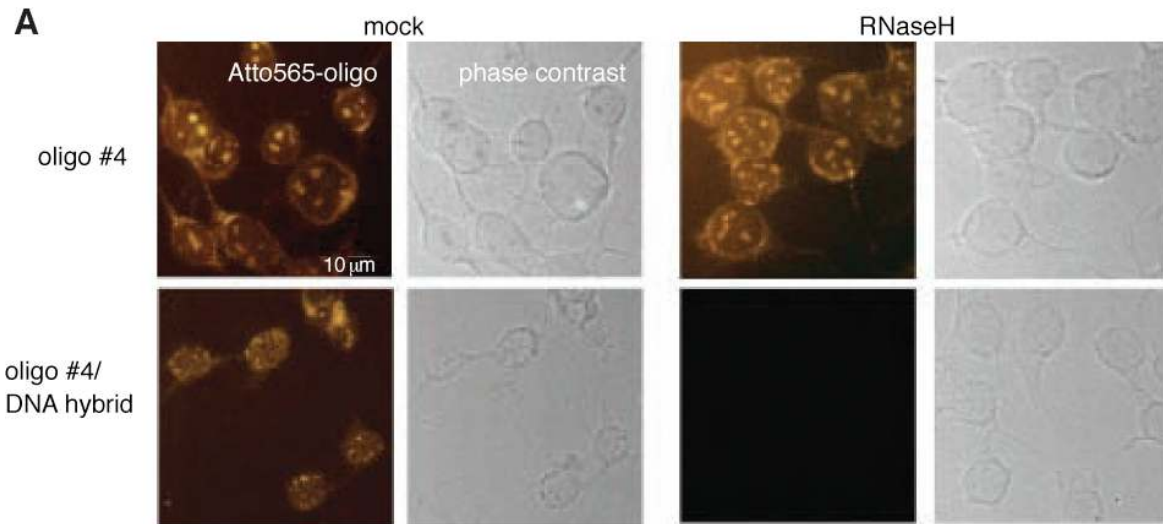
Schermelleh, L., Spada, F., Easwaran, H.P., Zolghadr, K., Margot, J.B., Cardoso, M.C., and Leonhardt, H. 2005. Trapped in action: direct visualization of DNA methyltransferase activity in living cells. *Nat. Methods* **2**: 751-756.

Strohner, R., Nemeth, A., Jansa, P., Hofmann-Rohrer, U., Santoro, R., Längst, G., and Grummt, I. 2001. NoRC - a novel member of mammalian ISWI-containing chromatin remodeling machines. *EMBO J.* **20**: 4892-4900.

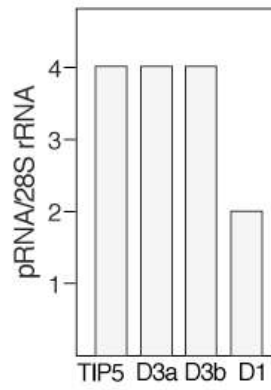








A



B

